The Astrophysical Journal Letters, 872:L23 (6pp), 2019 February 20 https://doi.org/10.3847/2041-8213/ab04b3

Seasonal Changes in Titan's Upper Haze Resulting from Saturn's Eccentric Orbit

E. J. L. Larson
Department of Organismic and Evolutionary Biology, Harvard University, 26 Oxford Street, Cambridge, MA 02138, USA
Received 2018 November 1; revised 2019 February 5; accepted 2019 February 6; published 2019 February 19

Abstract

Organic aerosols are produced high in the atmosphere of Titan by complex photochemical pathways starting from the dissociation of CH_4 by solar ultraviolet (UV) and N_2 by energetic particles. An end product of this photochemistry is the organic haze enshrouding Titan. The solar flux at Titan varies by about 20% between periapsis and apoapsis, thus we expect the dissociation of CH_4 and the total production of aerosols to have a similar seasonal dependence. The seasonal cycle in the haze production due to Saturn's orbital eccentricity is complicated by seasonal changes in dynamics and aerosol particle size due to Saturn's 27° obliquity. A 3D Titan general circulation model with fully coupled aerosol microphysics, the Titan Community Atmospheres Model, simulates the aerosol haze with and without aerosol production as a function of solar UV. Both simulations display an equatorial seasonal cycle in the haze above about 340 km; however, this cycle is amplified by a factor of 2 in the simulation with production as a function of solar UV. We compare the simulations with published estimates of haze extinction in the upper atmosphere. Current observations of the haze extinction at 400 km cannot distinguish between the two simulations, highlighting the difficulties that complicated dynamics in the upper atmosphere pose for trend detection.

Key words: planets and satellites: atmospheres

1. Introduction

Titan has a thick organic haze that forms through the dissociation of CH_4 and N_2 and ensuing complex photochemistry high in the atmosphere (Strobel 1974; Bar-Nun & Podolak 1979; Sagan & Khare 1979; Waite et al. 2007). Methane is predominantly dissociated by solar ultraviolet (UV) light, while nitrogen is dissociated from high energy particles from Saturn's magnetosphere (Yung et al. 1984; Fox & Yelle 1997). The absorption and scattering of light on the haze plays an important role in determining the temperature and dynamics in the atmosphere (McKay et al. 1991).

There are two orbital parameters that cause seasonality in the Saturnian system: eccentricity and obliquity. Saturn's 27° obliquity causes differential heating and cooling between the hemispheres on Titan. Titan's obliquity is 0.3° relative to Saturn's equatorial plane with an eccentricity of 0.029. The differential heating between the hemispheres drives a strong pole-to-pole overturning circulation on Titan. This seasonal cycle has been observed by *Cassini* in the temperature, winds, and trace gases (Teanby et al. 2012; Vinatier et al. 2015). Saturn's orbital eccentricity is 0.056, resulting in a difference between aphelion and perihelion of 11%. The solar flux falls off as the distance to the Sun squared, thus the magnitude of the seasonal cycle of the UV flux at Titan is about 22% due to Saturn's orbit around the Sun. Furthermore, Saturn's periapsis is observed at solar longitude (L_S) = 280° during Titan's northern winter and the apoapsis is at L_S = 98° during Titan's northern summer. Solar longitude is a measure of the seasonal phase of the Saturnian system with respect to the Sun, with the northern hemisphere spring equinox at L_S = 0°. Thus, the seasonal cycles induced by Saturn's obliquity and eccentricity are very nearly in phase with Titan's longer, but less intense, northern summers, and short and intense southern summers.

The production of aerosols in Titan's upper atmosphere is expected to have a seasonal cycle proportional to the UV flux and dissociation of methane. The obliquity is expected to change the hemispheric production of aerosols, but not the net aerosol production. Saturn's eccentricity, however, is expected to induce a seasonality in Titan's haze production, with more haze produced near periapsis during the southern summer. The differences in heating both between the hemispheres and the seasons creates dynamical feedback on the aerosol density (Teanby et al. 2012; Bezard et al. 2018).

Titan's aerosols are removed through settling and have a long atmospheric lifetime of over 10 Titan years or 300 Earth years (Larson et al. 2014), so we do not expect to see a signal of the seasonal production in the main haze layer. However, in the upper atmosphere of Titan where the atmosphere is much more tenuous, the haze has a relatively short residence time (Flasar et al. 1981). Above 340 km in our model the lifetime of the haze is less than a Titan season, or 7.4 Earth years. We hypothesize that the seasonal cycle of haze production may be detectable in Titan's upper atmosphere in limb profiles.

In this Letter, we simulate Titan's atmosphere with and without haze production as a function of solar insulation using a 3D general circulation model (GCM) that includes coupled aerosol microphysics. We compare our simulations with previously published limb profiles of haze extinction in Titan's upper atmosphere and assess them for evidence of a seasonal cycle in production.

2. Simulations of Seasonal Haze Production

Simulations of Titan's haze are computed with the Titan Community Atmospheres Model (TitanCAM; Friedson et al. 2009; Larson et al. 2014). This is a 3D GCM coupled to the CARMA aerosol microphysical model (Toon et al. 1992). Aerosols are produced in the model as 50 nm monomers input at the top of the atmosphere (Tomasko et al. 2008). The mean production rate, or mass flux at the top of the model, is 10^{-14} g cm^{-2} s^{-1}. Aerosols coagulate into fractal particles with a fractal dimension of 2 as they fall through the atmosphere. Their final size, of several hundred

nanometers, is limited by particle charging that acts to repel large particles from each other (Larson et al. 2014).

The model uses pressure levels as the vertical coordinate, with the top of the atmosphere pressure at 0.35 Pa. Titan's atmosphere inflates and contracts seasonally due to changing atmospheric temperatures, which convolutes our efforts to understand Titan's haze at altitude. *Cassini* observations show evidence of cooling in the equatorial regions of the upper atmosphere that is consistent with a decreasing solar constant (Achterberg et al. 2011; Bampasidis et al. 2012). This cooling accompanies a decreasing pressure at a constant altitude. Due to the seasonal cycle of upper atmospheric temperatures in this model, this pressure varies between 406 and 459 km. During the Huygens descent, the top of the model is at 455 km, about 10 km less than measured by the Huygens Atmospheric Structure Instrument (HASI) due to temperature differences (Fulchignoni et al. 2005). We restrict our analysis in this Letter to 400 km, which due to the varying altitude of the model occurs between the second and sixth level from the top of the model. Above the top of the model is a diffusive sponge layer. Our analysis does not rely on the topmost layer in the model and we consider it robust against boundary layer effects.

We compare two computer simulations, a control with constant haze production and an experimental run, where haze production is a function of orbital distance, and therefore, top of atmosphere (TOA) solar flux. The difference between these two simulations should be the effect of the seasonal haze production. The simulations were run for seven Titan years and we analyze the last two years in the simulations. We are not concerned about the lower atmosphere coming to a full equilibrium because of the short lifetimes of the upper atmosphere. The lifetime of aerosols in the upper atmosphere is less than a Titan season, and they come into a steady seasonal cycle in the second Titan year of the simulations.

The particles in Titan's atmosphere are believed to be fractal aggregates with a fractal dimension of 2 (Cabane et al. 1993; Tomasko et al. 2008). The fractal dimension describes how the mass of the particles scales with the radius, $m \propto r^{df}$. A fractal dimension of 3 is essentially a sphere and a fractal dimension of 1 resembles beads on a string. There are two interesting effects of having a fractal dimension of 2. One is that the particle fall velocity becomes independent of size above about 80 km. Thus, all the fractal particles in Titan's atmosphere fall at the same rate in the upper atmosphere (Larson et al. 2014). Another interesting property is that the extinction is roughly proportional to the local mass density (MD) of the haze (see the Appendix). Thus, the extinction is a good metric to use for analysis of haze production, which should be related to the total aerosol mass in the upper atmosphere.

The residence times of Titan's aerosols at each level of the atmosphere can be informative as they indicate where the seasonal cycle would disappear in the absence of strong mixing. Haze particles accumulate as they settle through the atmosphere because they fall slower in the lower atmosphere (fall velocity is proportional to one over the atmospheric density). Residence time is calculated as the cumulative aerosol mass from the TOA down toward the surface divided by the production rate. The seasonal cycle of haze production in Titan's atmosphere should be seen down to the altitude where the residence time is about a Titan season. For the production rate of 10^{-14} g cm^{-2} s^{-1}, this corresponds to about 340 km in the TitanCAM model. These results are corroborated by Figure 1, in which the autocorrelation of the haze number density in the upper atmosphere is plotted as a function of lag time in solar longitude (L_S) and pressure. The autocorrelation indicates how strongly a variable is correlated with its past self, i.e., correlated with itself after some elapsed or lag time. The contours in Figure 1 indicate the correlation between the haze number density time series and the time series shifted by a lag time. A strong seasonal cycle should show up as a cosine function in the autocorrelation. Half of a Titan year lag is expected to be negatively correlated with the current time, and a one year lag to be positively correlated. No correlation is indicative of no seasonal cycle. In the constant production simulation, the haze number density autocorrelation is weak, signaling no seasonal cycle. In the seasonal production simulation, the haze has a strong negative autocorrelation (-0.7) at half of a Titan year. This is expected due to the haze production being a function of Saturn's orbital distance. This pattern of autocorrelation persists down to about 340 km in the TitanCAM. Below this altitude, the seasonal signal of the haze production quickly diminishes as the haze accumulates.

Dynamics have seasonal cycles associated with Titan's obliquity that drive aerosol densities in the lower and upper atmosphere. The detached haze layer, a globally distributed layer of haze first observed by Voyager that is visually distinct from the main haze, is a good example of dynamics playing a dominant role in redistributing the haze (Rages & Pollack 1983; West et al. 2011). To distinguish between dynamic redistribution and production in the haze seasonal cycle, we need to assume our haze profile is high enough that the fall velocity is much greater than the vertical wind speed, which seems to be the case above about 340 km in this model. It should be noted that the TitanCAM model simulates the detached haze layer about 100 km lower than observed (Larson et al. 2015). Thus, in Titan's atmosphere a realistic limit is probably 400 km or more. The detached haze layer gives some guidance on where a seasonal production term could be detected as well. Although dynamical mixing could obscure the seasonal cycle even in the upper atmosphere (Rannou et al. 2004), the haze transport above the detached haze layer is dominated by particle fall velocities during most of the Titan year (Larson et al. 2015). However, the altitude of the detached haze layer also fluctuates and completely collapses a few (Earth) years after equinox (West et al. 2011, 2018). To limit the dynamical influence, we restrict our analysis of the simulated and observed haze to near 400 km.

The simulated aerosol haze at 400 km is indeed a function of Saturn's eccentricity as expected. Figure 2 displays the mean atmospheric and haze properties in the equatorial region (45°S–45°N) at 400 km in the model. The red and blue symbols indicate simulations with constant haze production and production scaled to the solar flux, respectively. The TOA UV flux that drives production of the haze is shown in Figure 2(A). The 400 km air temperature (Figure 2(B)) and pressure (Figure 2(C)) have the same seasonality as the solar flux; however, dynamical effects are present. Furthermore, we start to see feedback differences between the simulations from the heating and cooling of the aerosols. The seasonal production simulation has warmer temperatures during the northern winter, which inflate the atmosphere compared to the control simulation and decrease the vertical wind (Figure 2(D)). Due to the strong vertical gradient in aerosol abundance, vertical mixing greatly affects the local haze density. The

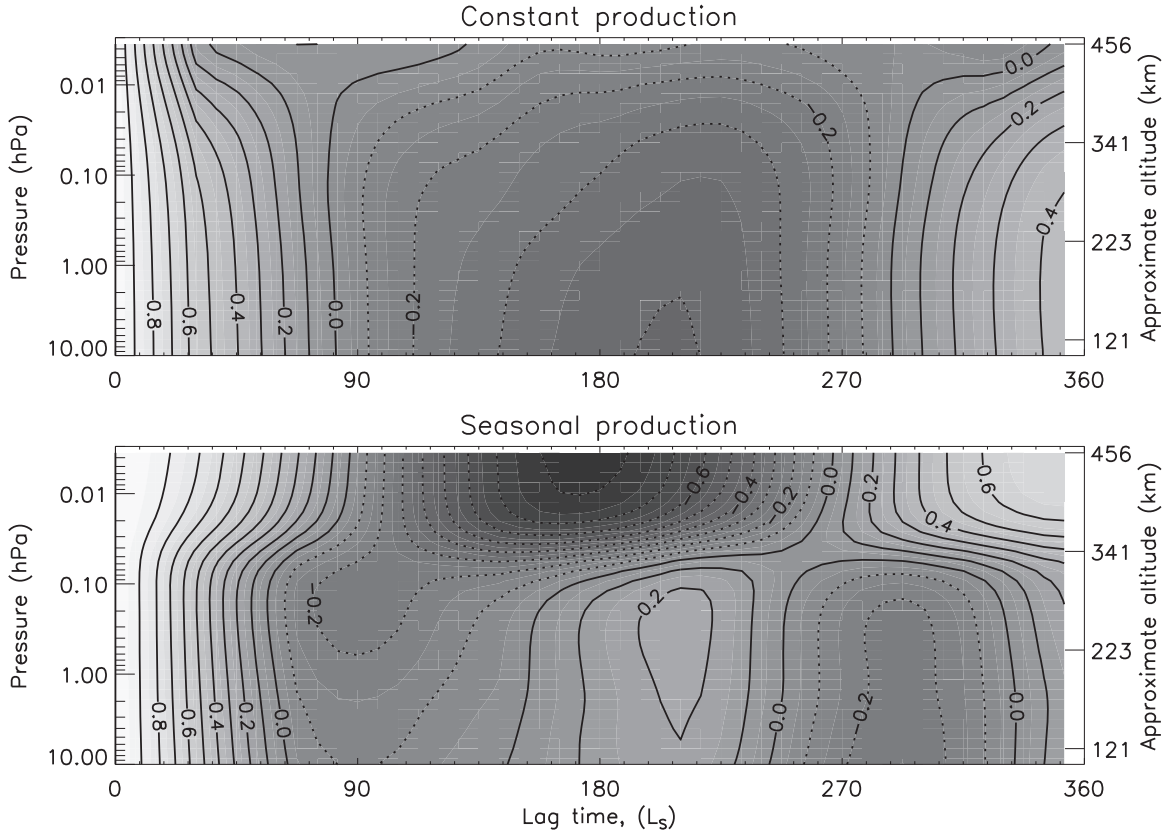

Figure 1. Autocorrelation of haze number density in TitanCAM. In the seasonal production simulation (bottom) there is a strong seasonal cycle of the haze number density above 340 km corresponding to the haze production rate.

vertical wind in Figure 2(D) does not include the expansion and contraction of the atmosphere, indicated on the right axis of Figure 2(C). The atmospheric contraction after equinox is consistent with the fall of the detached haze layer observed by West et al. (2011, 2018). The variation in pressure at 400 km follows the same trend as the haze observed by *Cassini*: stable in altitude during the northern winter up to the equinox and decreasing quickly after. The vertical wind also does not represent the total particle movement, which is the vertical wind plus the particle fall velocity. The fall velocities are generally larger than the vertical wind speed above about 350 km (Larson et al. 2014).

The particle number density (Figure 2(E)) displays a strong seasonal cycle consistent with the solar flux and production. The particle effective radius (Figure 2(F)) is controlled by coagulation and has a more complicated seasonal cycle, with the seasonal production simulation tending to have a higher particle radius than the control simulation. The MD (Figure 2(G)) and 525 nm extinction (Figure 2(H)) are essentially a convolution of the number density and effective radius and have a strong seasonal cycle consistent with Saturn's eccentricity. The seasonal cycle of the haze in the constant production simulation is caused by dynamical movements alone. The seasonal cycle of the experimental simulation is due to the combination of the seasonal production term and dynamics. The impact of the seasonal haze production on the MD and extinction is evident in the fractional change shown on the right axis of Figures 2(G) and (H). The effect of Saturn's eccentricity on haze production accounts for about half of the magnitude of the seasonal cycle in the haze extinction and MD (Figures 2(G), (H)) in the experimental simulation. The fractional change in the 400 km haze density is about ±20% of the mean (Figures 2(G), (H)), which is larger than predicted. The UV flux varies by ±11% of the mean. The difference is due to dynamical feedback. If the two simulations are compared at similar pressure levels instead of altitudes, the fractional change between the simulations is about ±10%, consistent with the difference in haze production. Note that the haze extinction and MD display very similar seasonal cycles supporting our earlier claim that the extinction is a good proxy for the MD and thus production rate (Appendix).

3. Analysis of Haze Profiles

We analyze several previously published limb profiles of haze extinction for evidence of seasonality in net haze production (Rages & Pollack 1983; West et al. 2011, 2018). The extinction values in these studies were scaled to 525 nm using scaling coefficients; specifically, the 343 nm extinction values are multiplied by 0.5 (Larson et al. 2014). These papers have mostly focused on the detached haze layer and its seasonal cycle in altitude. We fit an exponential plus a Gaussian term representing the gap in the haze to the haze extinction profiles above 300 km. This model fits well and allows us to determine the scale height (H_0) of the upper atmosphere and the extinction in the absence of the gap in the haze. By fitting the observed haze profiles, we obtain an estimate of the haze at 400 km that is dependent on the entire upper atmospheric column and less sensitive to the detached haze layer. This should provides a signal that is more consistent with the haze production than the observed 400 km haze extinction values. However, the two are very similar outside of

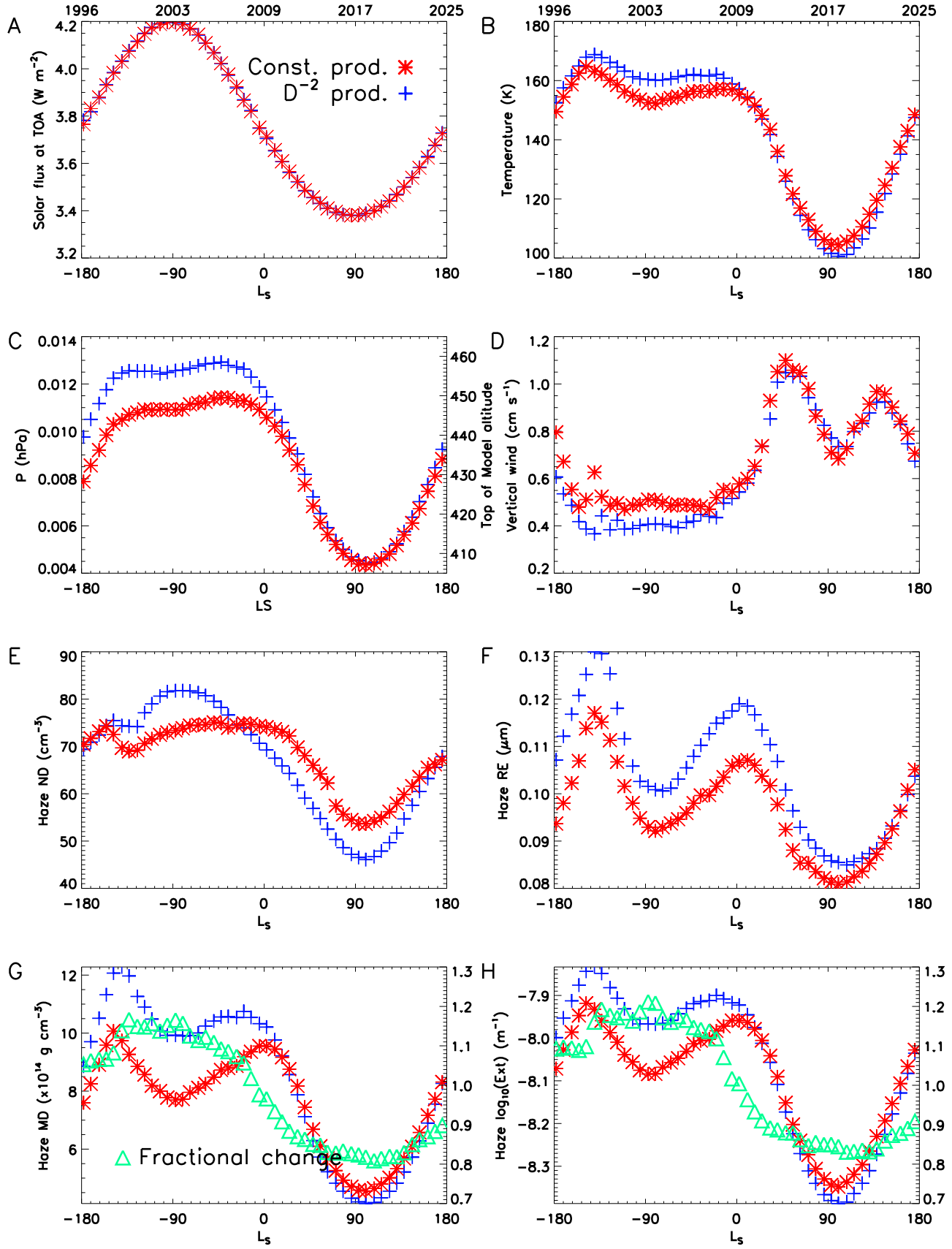

Figure 2. Atmospheric and aerosol properties over two Titan years at 400 km in the TitanCAM model. The simulation with constant haze production is in red, and the simulation with haze production proportional to D^{-2}, where D is the distance to the Sun, is in blue. The fractional change in panel (G) and (H) is the seasonal divided by the constant production simulations. This indicates how much of the seasonal cycle in extinction and haze mass are due to the seasonal production terms.

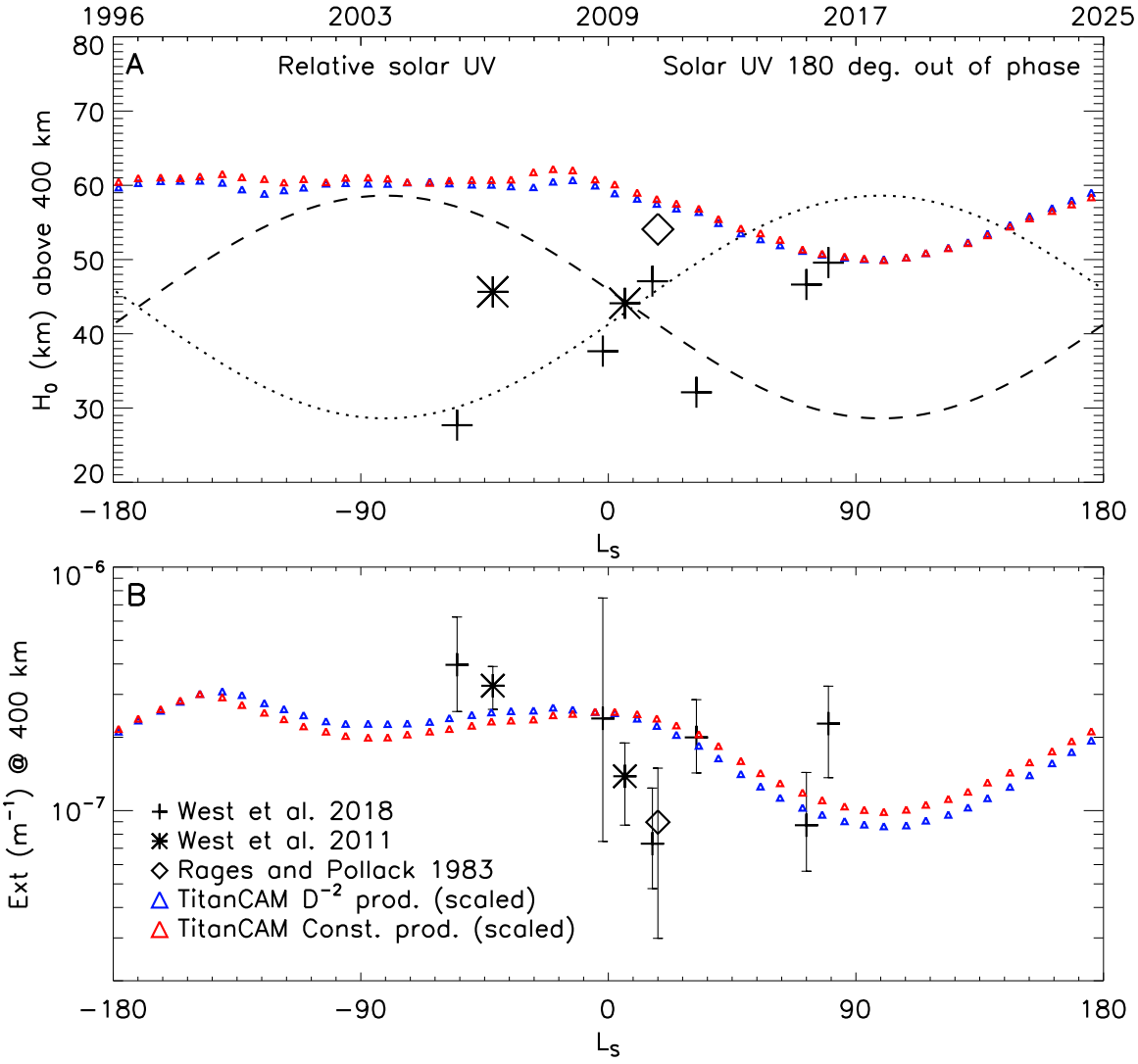

Figure 3. (A) Seasonal cycle of the observed and simulated aerosol scale heights above 400 km along with dashed and dotted lines showing the relative solar insolation and solar insolation 180° out of phase, respectively. (B) Observed and simulated 525 nm extinction of the haze at 400 km.

the detached haze layer. The scale heights of these profiles along with the TitanCAM scale heights can be seen in Figure 3(A). The observed scale heights vary between 28 and 54 km. The TitanCAM scale heights are larger than the observations ranging between 50 and 62 km. Furthermore, the simulated scale heights have a similar seasonal cycle to the solar flux, whereas the limb profile scale heights do not. As the upper atmosphere warms near periapsis, it expands, and the scale height is expected to increase (Figure 2(C)). Thus, we would expect the scale height to have a similar seasonal cycle as the solar flux, as it does in the simulations. We do not detect a strong seasonal cycle in the observed scale heights. This mismatch between observations and the model may suggest that dynamics play a more important role than previously thought above 400 km. There seems to be evidence of wavelike structures in extinction profiles in West et al. (2018) that are well above the detached haze layer. A similar wavelike structure was detected by Porco et al. (2005) in high-resolution images near Titan's poles. Furthermore, Koskinen et al. (2011) showed evidence of vertical structure including another detached layer above 700 km in altitude. The upper level dynamics that potentially create this vertical structure can transport haze and affect the scale height.

The simulated extinction at 400 km shows a seasonal pattern consistent with production that is proportional to the solar flux (Figures 2(H), 3(B)). The extinction from the limb profiles shows a similar seasonal pattern; however, the observations, which have a very low signal-to-noise ratio, still have a large uncertainty compared to the difference between the simulations, which is on the order of tens of percent. Thus, the observed extinctions are not indistinguishable from a constant production rate. The model has low interannual variability at these altitudes and the difference between successive years of simulations is ±2%, or roughly the size of the symbols used to represent the simulations in Figure 3. The seasonal pattern of the observed limb extinctions has a high resemblance to the seasonal pattern of the detached haze observed by *Cassini*. This suggests that it is not just the detached haze or its associated gap that falls through the atmosphere, but the whole column of haze that descends after equinox.

4. Conclusions

Model results indicate substantial changes in high altitude haze due to seasonal dynamics and the seasonal production of aerosols. The dynamical changes result from both Saturn's eccentricity and obliquity. About half of the seasonal change in haze extinction at 400 km is due to haze production being proportional to the solar flux. Dynamical feedback is responsible for the other half of the modeled seasonal cycle in haze extinction.

Observing these changes in haze production, however, is difficult. Several factors could limit the ability to accurately estimate upper atmosphere haze extinction and MD, including: (1) current limitations with observations including signal-to-noise ratio and varying phase angles, (2) vertical transport that is unaccounted for in the model, (3) changing particle properties such as size or composition, and (4) latitudinal transport. Because aerosol density broadly reflects atmospheric density, it decreases exponentially with altitude. Thus, modest vertical movements could result in large changes in haze extinction at a particular altitude. Modeling suggests that a signal due to eccentricity is possible to detect, however, the observations do not yet support this theory.

Latitudinal transport plays an important role in redistributing the upper atmospheric haze. While this Letter primarily focuses on the equatorial changes, it should be noted that the poles undergo strong seasonality due to Titan's obliquity. In general, the haze is transported from the summer to the winter hemisphere, where it descends and accumulates at the pole creating the polar hood. This seasonality is not symmetric, however, due to Saturn's eccentricity that affects both the magnitude of the overturning circulation and the haze production. The effect of eccentricity on the production creates a larger amount of haze mass during the southern summer that is available to be transported to the winter pole. This, combined with the more intense circulation, creates a northern polar hood with higher haze MD than the southern polar hood.

The extended period of stable conditions in temperature, pressure, vertical velocity, and haze number density observed during the northern winter are not predicted by this model during the northern summer. As yet, the symmetry between the seasons can only be modeled or observed from Earth. Despite the 13 years of mission, *Cassini* only observed Titan during less than half an orbit, and the behavior in its upper atmosphere during the northern summer and fall are yet completely unknown.

Appendix

For a monodisperse haze distribution,

$$\mathrm{Ext} = Q_{\mathrm{ext}}\,\pi\, r_{\mathrm{f}}{}^2\, N \tag{1}$$

where ext is the extinction, Q_{ext} is the extinction (scattering + absorption) coefficient, r_{f} is the fractal radius, and N is the particle number density. The extinction coefficient is calculated using the mean field approximation (Botet et al. 1997). The number density is equal to MD divided by the particle mass (m_{p}),

$$N = \mathrm{MD}/m_{\mathrm{p}}. \tag{2}$$

The particle mass is equal to the particle density (ρ_{p}) times the volume of the particle. Here r_{s} is the equivalent mass spherical radius of the particles.

$$m_{\mathrm{p}} = \rho_{\mathrm{p}} 4/3\pi\, r_{\mathrm{s}}{}^3. \tag{3}$$

By definition, r_{s} is related to the fractal and monomer radii for a fractal dimension of 2 by the following:

$$r_{\mathrm{f}}{}^2 = r_{\mathrm{s}}{}^3/r_{\mathrm{mon}} \tag{4}$$

where r_{f} is the fractal radius, and r_{mon} is the monomer radius. The particle mass is therefore

$$m_{\mathrm{p}} = \rho_{\mathrm{p}} 4/3\pi\, r_{\mathrm{mon}}\, r_{\mathrm{f}}{}^2. \tag{5}$$

By substituting the particle mass as a function of particle density and radii into Equation (2) and substituting the number density into Equation (1), we can write the extinction as a function of the MD and constants as follows:

$$\mathrm{Ext} = Q_{\mathrm{ext}} (\rho_{\mathrm{p}} 4/3\, r_{\mathrm{mon}})^{-1}\, \mathrm{MD}. \tag{6}$$

In this equation, the extinction is only weakly dependent on particle size through the extinction coefficients. Thus, the extinction is directly related to the haze production.

References

Achterberg, R. K., Gierasch, P. J., Conrath, B. J., et al. 2011, Icar, 211, 686
Bampasidis, G., Coustenis, A., Achterberg, R. K., et al. 2012, ApJ, 760, 144
Bar-Nun, A., & Podolak, M. 1979, Icar, 38, 115
Bezard, B., Vinatier, S., & Achterberg, R. K. 2018, Icar, 302, 437
Botet, R., Rannou, P., & Cabane, M. 1997, ApOpt, 36, 8791
Cabane, M., Rannou, P., Chassefiere, E., & Israel, G. 1993, PSS, 41, 257
Flasar, F. M., Samuelson, E., & Conrath, B. J. 1981, Natur, 292, 693
Fox, J. L., & Yelle, R. V. 1997, GeoRL, 24, 2179
Friedson, A. J., West, R. A., Wilson, E., et al. 2009, PSS, 57, 1931
Fulchignoni, M., Ferri, F., Angrilli, F., et al. 2005, Natur, 483, 785
Koskinen, T. T., Yelle, R. V., Snowden, D. S., et al. 2011, Icar, 216, 506
Larson, E. J. L., Toon, O. B., & Friedson, A. J. 2014, Icar, 243, 400
Larson, E. J. L., Toon, O. B., West, R. A., & Friedson, A. J. 2015, Icar, 254, 122
McKay, C. P., Pollack, J. B., & Courtin, R. 1991, Sci, 253, 1118
Porco, C. C., Baker, E., Barbara, J., et al. 2005, Natur, 434, 159
Rages, K., & Pollack, J. B. 1983, Icar, 55, 50
Rannou, P., Hourdin, F., McKay, C. P., et al. 2004, Icar, 170, 443
Sagan, C., & Khare, B. N. 1979, Natur, 277, 102
Strobel, D. 1974, Icar, 21, 466
Teanby, N. A., Irwin, P. G. J., Nixon, C. A., et al. 2012, Natur, 491, 732
Tomasko, M. G., Doose, L., Engel, S., et al. 2008, PSS, 56, 669
Toon, O. B., McKay, C. P., Griffith, C. A., et al. 1992, Icar, 95, 24
Vinatier, S., Bezard, B., Lebbonois, S., et al. 2015, Icar, 250, 95
Waite, J. H., Young, D. T., Cravens, T. E., et al. 2007, Sci, 316, 870
West, R. A., Balloch, J., Dumont, P., et al. 2011, GeoRL, 38, L06204
West, R. A., Seignovert, B., Rannou, P., et al. 2018, NatAs, 2, 495
Yung, Y. L., Allen, M., & Pinto, J. P. 1984, ApJS, 55, 465